PERGAMON

Automatica 36 (2000) 363–378

www.elsevier.com/locate/automatica

Drum-boiler dynamics☆

K.J. Åström[a,*], R.D. Bell[b]

[a]Department of Automatic Control, Lund Institute of Technology, Box 118, S-221 00 Lund, Sweden
[b]Department of Computing, School of Mathematics, Physics, Computing and Electronics, Macquarie University, New South Wales 2109, Australia

Received 2 October 1998; revised 7 March 1999; received in final form 8 June 1999

Abstract

A nonlinear dynamic model for natural circulation drum-boilers is presented. The model describes the complicated dynamics of the drum, downcomer, and riser components. It is derived from first principles, and is characterized by a few physical parameters. A strong effort has been made to strike a balance between fidelity and simplicity. Results from validation of the model against unique plant data are presented. The model describes the behavior of the system over a wide operating range. © 2000 Elsevier Science Ltd. All rights reserved.

1. Introduction

There are dramatic changes in the power industry because of deregulation. One consequence of this is that the demands for rapid changes in power generation is increasing. This leads to more stringent requirements on the control systems for the processes. It is required to keep the processes operating well for large changes in the operating conditions. One way to achieve this is to incorporate more process knowledge into the systems. There has also been a significant development of methods for model-based control, see Garcia, Prett and Morari (1989), Qin and Badgwell (1997) and Mayne, Rawlings and Rao (1999). Lack of good nonlinear process models is a bottleneck for using model-based controllers. For many industrial processes there are good static models used for process design and steady-state operation. By using system identification techniques it is possible to obtain black box models of reasonable complexity that describe the system well in specific operating conditions. Neither static models nor black box models are suitable for model-based control. Static design models are quite complex and they do not capture dynamics. Black box models are only valid for specific operating conditions.

This paper presents a nonlinear model for steam generation systems which are a crucial part of most power plants. The goal is to develop moderately complex nonlinear models that capture the key dynamical properties over a wide operating range. The models are based on physical principles and have a small number of parameters; most of which are determined from construction data. Particular attention has been devoted to model drum level dynamics well. Drum level control is an important problem for nuclear as well as conventional plants, see Kwatny and Berg (1993) and Ambos, Duc and Falinower (1996). In Parry, Petetrot and Vivien (1995) it is stated that about 30% of the emergency shutdowns in French PWR plants are caused by poor level control of the steam water level. One reason is that the control problem is difficult because of the complicated shrink and swell dynamics. This creates a nonminimum phase behavior which changes significantly with the operating conditions.

Since boilers are so common there are many modeling efforts. There are complicated models in the form of large simulation codes which are based on finite element approximations to partial differential equations. Although such models are important for plant design, simulators, and commissioning, they are of little interest for control design because of their complexity. Among the early work on models suitable for control we can mention Profos (1955, 1962), Chien, Ergin, Ling and Lee (1958), de Mello (1963), Nicholson (1964), Thompson (1964),

☆This paper was presented at IFAC 13th World Congress, San Francisco, CA, 1996. This paper was recommended for publication in revised form by Associate Editor T.A. Johansen under the direction of Editor S. Skogestad.

* Corresponding author. Tel.: 00-46-46-222-8781; fax: 00-46-46-138-8118.

E-mail address: kja@control.lth.se (K. J. Åström)

0005-1098/00/$ - see front matter © 2000 Elsevier Science Ltd. All rights reserved.
PII: S0005-1098(99)00171-5

Quazza (1968, 1970), Caseau and Godin (1969), Kwan and Andersson (1970), McDonald and Kwatny (1970), Speedy, Bell and Goodwin (1970), Dolezal and Varcop (1970), McDonald, Kwatny and Spare (1971), Eklund (1971), Åström and Eklund (1972), Åström (1972), Bell (1973), Borsi (1974), Lindahl (1976), Tyssø, Brembo and Lind (1976), Bell, Rees and Lee (1977) and Morton and Price (1977). Boiler modeling is still of substantial interest. Among more recent publications we can mention Maffezzoni (1988, 1992, 1996), Klefenz (1986), Jarkovsky, Fessl and Medulova (1988), Unbehauen and Kocaarslan (1990), Höld (1990), Na and No (1992), Kwatny and Berg (1993), Na (1995).

The work presented in this paper is part of an ongoing long-range research project that started with Eklund (1971) and Bell (1973). The work has been a mixture of physical modeling, system identification and model simplification. It has been guided by plant experiments in Sweden and Australia. The unique measurements reported in Eklund (1971) have been particularly useful. A sequence of experiments with much excitation were performed on a boiler over a wide range of operating conditions. Because of the excitation used, these measurements reveal much of the dynamics of interest for control. Results of system identification experiments indicated that the essential dynamics could in fact be captured by simple models, see Åström and Eklund (1972). However, it has not been easy to find first principles models of the appropriate complexity. Many different approaches have been used. We have searched for the physical phenomena that yield models of the appropriate complexity. Over the years the models have changed in complexity both increasing and decreasing; empirical coefficients have been replaced by physical parameters as our understanding of the system has increased. The papers Åström and Eklund (1972, 1975), Åström and Bell (1988, 1993) and Bell and Åström (1996) describe how the models have evolved. The models have also been used for control design, see Miller, Bentsman, Drake, Fahkfahk, Jolly, Pellegrinetti and Tse (1990), Pellegrinetti, Bentsman and Polla (1991), and Cheng and Rees (1997). Models based on a similar structure have been used for simulation and control of deaerators, see Lu, Bell and Rees (1997), and nuclear reactors, see Yeung and Chan (1990), Höld (1990), Irving, Miossec and Tassart (1980), Parry et al. (1995), Menon and Parlos (1992), Thomas, Harrison and Hollywell (1985), Schneider and Boyd (1985) and Kothare, Mettler, Morari, Bendotti and Falinower (1999).

2. Global mass and energy balances

A schematic picture of a boiler system is shown in Fig. 1. The heat, Q, supplied to the risers causes boiling. Gravity forces the saturated steam to rise causing a circulation in the riser-drum-downcomer loop. Feedwater, q_f, is supplied to the drum and saturated steam, q_s, is taken from the drum to the superheaters and the turbine. The presence of steam below the liquid level in the drum causes the shrink-and-swell phenomenon which makes level control difficult. In reality the system is much more complicated than shown in the figure. The system has a complicated geometry and there are many downcomer and riser tubes. The outflow from the risers passes through a separator to separate the steam from the water. In spite of the complexity of the system it turns out that its gross behavior is well captured by global mass and energy balances.

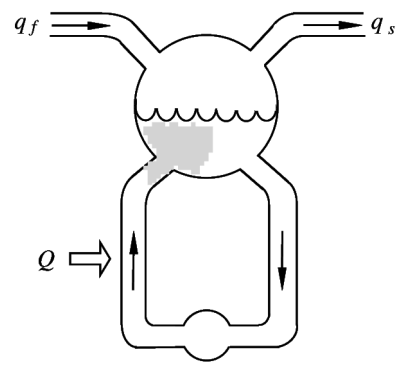

Fig. 1. Schematic picture of the boiler.

A key property of boilers is that there is a very efficient heat transfer due to boiling and condensation. All parts of the system which are in contact with the saturated liquid–vapor mixture will be in thermal equilibrium. Energy stored in steam and water is released or absorbed very rapidly when the pressure changes. This mechanism is the key for understanding boiler dynamics. The rapid release of energy ensures that different parts of the boiler change their temperature in the same way. For this reason the dynamics can be captured by models of low order. Drum pressure and power dynamics can, in fact, be represented very well with first-order dynamics as shown in Åström and Eklund (1972). At first it is surprising that the distributed effects can be neglected for a system with so large physical dimensions.

Typical values of stored energy for two different boilers are given in Table 1. The P16-G16 plant is a 160 MW unit in Sweden and the Eraring plant is a 660 MW unit in Australia. The ratio of the energy stored in the metal to that stored in the water is approximately 1 for P16-G16 and 4 for the Eraring unit.

The numbers in Table 1 also give a measure of the time it takes to deplete the stored energy at the generated rate. Although the total normalized stored energy is approximately the same for both plants the fraction of the energy stored in water is much smaller for the larger plant. This results in larger variations in water level for the larger plant under proportionally

Table 1
Energy stored in metal, water, and steam for two boilers operating at rated pressure and temperature but at different power generation conditions. The values are normalized with the power at the operating conditions. The unit is J/W = s, the entries can thus be interpreted as time constants for the different storage mechanisms

Boiler	Metal	Water	Steam	Total
P16-G16 80 MW	641	739	64	1444
P16-G16 160 MW	320	333	37	690
Eraring 330 MW	1174	303	60	1537
Eraring 660 MW	587	137	35	759

similar operating condition changes. This implies that the level control problem is more difficult for large boilers.

2.1. Balance equations

Much of the behavior of the system is captured by global mass and energy balances. Let the inputs to the system be the heat flow rate to the risers, Q, the feedwater mass flow rate, q_f, and the steam mass flow rate, q_s. Furthermore, let the outputs of the system be drum pressure, p, and drum water level, ℓ. This way of characterizing the system is convenient for modeling. For simulation and control it is necessary to account for the fact that mass flow rate q_s depends on the pressure by modeling the turbine and the superheaters.

To write the equations, let V denote volume, ϱ denotes specific density, u specific internal energy, h specific enthalpy, t temperature and q mass flow rate. Furthermore, let subscripts s, w, f and m refer to steam, water, feedwater, and metal, respectively. Sometimes, for clarification, we need a notation for the system components. For this purpose we will use double subscripts where t denotes total system, d drum and r risers. The total mass of the metal tubes and the drum is m_t and the specific heat of the metal is C_p.

The global mass balance is

$$\frac{d}{dt}[\varrho_s V_{st} + \varrho_w V_{wt}] = q_f - q_s \tag{1}$$

and the global energy balance is

$$\frac{d}{dt}[\varrho_s u_s V_{st} + \varrho_w u_w V_{wt} + m_t C_p t_m] = Q + q_f h_f - q_s h_s. \tag{2}$$

Since the internal energy is $u = h - p/\varrho$, the global energy balance can be written as

$$\frac{d}{dt}[\varrho_s h_s V_{st} + \varrho_w h_w V_{wt} - pV_t + m_t C_p t_m] = Q + q_f h_f - q_s h_s, \tag{3}$$

where V_{st} and V_{wt} represent the total steam and water volumes, respectively. The total volume of the drum, downcomer, and risers, V_t is

$$V_t = V_{st} + V_{wt}. \tag{4}$$

The metal temperature t_m can be expressed as a function of pressure by assuming that changes in t_m are strongly correlated to changes in the saturation temperature of steam t_s and thus also to changes in p. Simulations with models having a detailed representation of the temperature distribution in the metal show that the steady-state metal temperature is close to the saturation temperature and that the temperature differences also are small dynamically. The right-hand side of Eq. (3) represents the energy flow to the system from fuel and feedwater and the energy flow from the system via the steam.

2.1.1. A second-order model

Eqs. (1), (3), and (4) combined with saturated steam tables yields a simple boiler model. Mathematically, the model is a differential algebraic system. Such systems can be entered directly in modeling languages such as Omola and Modelica and it can be simulated directly using Omsim, see Mattsson, Andersson and Åström (1993) or Dymola. In this way we avoid making manual operations which are time consuming and error prone.

We will, however, make manipulations of the model to obtain a state model. This gives insight into the key physical mechanisms that affect the dynamic behavior of the system. There are many possible choices of state variables. Since all parts are in thermal equilibrium it is natural to choose drum pressure p as one state variable. This variable is also easy to measure. Using saturated steam tables, the variables ϱ_s, ϱ_w, h_s, and h_w can then be expressed as functions of steam pressure. The second state variable can be chosen as the total volume of water in the system, i.e. V_{wt}. Using Eq. (4) and noting that V_t is constant, V_{st} can then be eliminated from Eqs. (1) and (3)

to give the following state equations:

$$e_{11}\frac{\mathrm{d}V_{\mathrm{wt}}}{\mathrm{d}t} + e_{12}\frac{\mathrm{d}p}{\mathrm{d}t} = q_{\mathrm{f}} - q_{\mathrm{s}}$$

$$e_{21}\frac{\mathrm{d}V_{\mathrm{wt}}}{\mathrm{d}t} + e_{22}\frac{\mathrm{d}p}{\mathrm{d}t} = Q + q_{\mathrm{f}}h_{\mathrm{f}} - q_{\mathrm{s}}h_{\mathrm{s}}, \tag{5}$$

where

$$e_{11} = \varrho_{\mathrm{w}} - \varrho_{\mathrm{s}}$$

$$e_{12} = V_{\mathrm{st}}\frac{\partial\varrho_{\mathrm{s}}}{\partial p} + V_{\mathrm{wt}}\frac{\partial\varrho_{\mathrm{w}}}{\partial p}$$

$$e_{21} = \varrho_{\mathrm{w}}h_{\mathrm{w}} - \varrho_{\mathrm{s}}h_{\mathrm{s}}$$

$$e_{22} = V_{\mathrm{st}}\left(h_{\mathrm{s}}\frac{\partial\varrho_{\mathrm{s}}}{\partial p} + \varrho_{\mathrm{s}}\frac{\partial h_{\mathrm{s}}}{\partial p}\right) + V_{\mathrm{wt}}\left(h_{\mathrm{w}}\frac{\partial\varrho_{\mathrm{w}}}{\partial p} + \varrho_{\mathrm{w}}\frac{\partial h_{\mathrm{w}}}{\partial p}\right) - V_{\mathrm{t}} + m_{\mathrm{t}}C_p\frac{\partial t_{\mathrm{s}}}{\partial p}. \tag{6}$$

This model captures the gross behavior of the boiler quite well. In particular it describes the response of drum pressure to changes in input power, feedwater flow rate, and steam flow rate very well. The model does, however, have one serious deficiency. Although it describes the total water in the system it does not capture the behavior of the drum level because it does not describe the distribution of steam and water in the system.

2.2. Further simplifications

Additional simplifications can be made if we are only interested in the drum pressure. Multiplying (1) by h_{w} and subtracting the result from (3) gives

$$h_{\mathrm{c}}\frac{\mathrm{d}}{\mathrm{d}t}(\varrho_{\mathrm{s}}V_{\mathrm{st}}) + \varrho_{\mathrm{s}}V_{\mathrm{st}}\frac{\mathrm{d}h_{\mathrm{s}}}{\mathrm{d}t} + \varrho_{\mathrm{w}}V_{\mathrm{wt}}\frac{\mathrm{d}h_{\mathrm{w}}}{\mathrm{d}t} - V_{\mathrm{t}}\frac{\mathrm{d}p}{\mathrm{d}t} + m_{\mathrm{t}}C_p\frac{\mathrm{d}t_{\mathrm{s}}}{\mathrm{d}t} = Q - q_{\mathrm{f}}(h_{\mathrm{w}} - h_{\mathrm{f}}) - q_{\mathrm{s}}h_{\mathrm{c}},$$

where $h_{\mathrm{c}} = h_{\mathrm{s}} - h_{\mathrm{w}}$ is the condensation enthalpy.

If the drum level is controlled well the variations in the steam volume are small. Neglecting these variations we get the following approximate model:

$$e_1\frac{\mathrm{d}p}{\mathrm{d}t} = Q - q_{\mathrm{f}}(h_{\mathrm{w}} - h_{\mathrm{f}}) - q_{\mathrm{s}}h_{\mathrm{c}}, \tag{7}$$

where

$$e_1 = h_{\mathrm{c}}V_{\mathrm{st}}\frac{\partial\varrho_{\mathrm{s}}}{\partial p} + \varrho_{\mathrm{s}}V_{\mathrm{st}}\frac{\partial h_{\mathrm{s}}}{\partial p} + \varrho_{\mathrm{w}}V_{\mathrm{wt}}\frac{\partial h_{\mathrm{w}}}{\partial p} + m_{\mathrm{t}}C_p\frac{\partial t_{\mathrm{s}}}{\partial p} - V_{\mathrm{t}}.$$

The term V_{t} in e_1 comes from the relation between internal energy and enthalpy. This term is often neglected in modeling, see Denn (1987). The relative magnitudes of the terms of e_1 for two boilers are given in Table 2. The terms containing $\partial h_{\mathrm{w}}/\partial p$ and $\partial t_{\mathrm{s}}/\partial p$ are the dominating terms in the expression for e_1. This implies that the changes in energy content of the water and metal masses are the physical phenomena that dominate the dynamics of drum pressure. A good approximation of e_1 is

$$e_1 \approx \varrho_{\mathrm{w}}V_{\mathrm{wt}}\frac{\partial h_{\mathrm{w}}}{\partial p} + mC_p\frac{\partial t_{\mathrm{s}}}{\partial p}.$$

Table 2 gives good insight into the physical mechanisms that govern the behavior of the system. Consider for example the situation when the pressure changes. The change in stored energy for this pressure change will be proportional to the numbers in the last two columns of the table. The column for the steam ($\partial h_{\mathrm{s}}/\partial p$) indicates that energy changes in the steam are two orders of magnitude smaller than the energy changes in water and metal. The balance of the change in energy is used in the boiling or condensation of steam. The condensation flow rate is

$$q_{\mathrm{ct}} = \frac{h_{\mathrm{w}} - h_{\mathrm{f}}}{h_{\mathrm{c}}}q_{\mathrm{f}} + \frac{1}{h_{\mathrm{c}}}\left(\varrho_{\mathrm{s}}V_{\mathrm{st}}\frac{\mathrm{d}h_{\mathrm{s}}}{\mathrm{d}t} + \varrho_{\mathrm{w}}V_{\mathrm{wt}}\frac{\mathrm{d}h_{\mathrm{w}}}{\mathrm{d}t} - V_{\mathrm{t}}\frac{\mathrm{d}p}{\mathrm{d}t} + m_{\mathrm{t}}C_p\frac{\mathrm{d}t_{\mathrm{s}}}{\mathrm{d}t}\right). \tag{8}$$

Model (7) captures the responses in drum pressure to changes in heat flow rate, feedwater flow rate, feedwater temperature and steam flow rate very well. An attractive feature is that all parameters are given by steam tables and construction data. The equation gives good insight into the nonlinear characteristics of the pressure

Table 2
Numerical values of the terms of the coefficient e_1 at normal operating pressure

Boiler	$h_{\mathrm{c}}V_{\mathrm{st}}\frac{\partial\varrho_{\mathrm{s}}}{\partial p}$	$\varrho_{\mathrm{s}}V_{\mathrm{st}}\frac{\partial h_{\mathrm{s}}}{\partial p}$	$\varrho_{\mathrm{w}}V_{\mathrm{wt}}\frac{\partial h_{\mathrm{w}}}{\partial p}$	$m_{\mathrm{t}}C_p\frac{\partial t_{\mathrm{s}}}{\partial p}$	V_{t}
P16-G16 80 MW	360	− 40	2080	1410	85
P16-G16 160 MW	420	− 40	1870	1410	85
Eraring 330 MW	700	− 270	2240	4620	169
Eraring 660 MW	810	− 270	2020	4620	169

response, since both e_1 and the enthalpies on the right-hand side of the equation depend on the operating pressure. To obtain a complete model for simulating the drum pressure a model for the steam valve has to be supplied.

The pressure model given by Eq. (7) is similar to the models in de Mello (1963), Quazza (1968), Åström and Eklund (1972), and Maffezzoni (1988). Models similar to (7) are included in most boiler models. Since model (7) is based on global mass and energy balances it cannot capture phenomena that are related to the distribution of steam and water in the boiler. Therefore it cannot model the drum level.

3. Distribution of steam in risers and drum

To obtain a model which can describe the behavior of the drum level we must account for the distribution of steam and water in the system. The redistribution of steam and water in the system causes the shrink-and-swell effect which causes the nonminimum-phase behavior of level dynamics, see Kwatny and Berg (1993). One manifestation is that the level will increase when the steam valve is opened because the drum pressure will drop, causing a swelling of the steam bubbles below the drum level.

The behavior of two phase flow is very complicated and is typically modeled by partial differential equations, see Kutateladze (1959) and Heusser (1996). A key contribution of this paper is that it is possible to derive relatively simple lumped parameter models that agree well with experimental data.

3.1. Saturated mixture quality in a heated tube

We will start by discussing the dynamics of water and steam in a heated tube. Consider a vertical tube with uniform heating. Let ϱ be the density of the steam–water mixture. Furthermore let q be the mass flow rate, A the area of the cross section of the tube, V the volume, h the specific enthalpy, and Q the heat supplied to the tube. All quantities are distributed in time, t, and space, z. Assume for simplicity that all quantities are the same in a cross section of the tube. The spatial distribution can then be captured by one coordinate z and all variables are then functions of z and time t.

The mass and energy balances for a heated section of the tube are

$$A\frac{\partial \varrho}{\partial t} + \frac{\partial q}{\partial z} = 0,$$

$$\frac{\partial \varrho h}{\partial t} + \frac{1}{A}\frac{\partial qh}{\partial z} = \frac{Q}{V}.$$

Let α_m denote the mass fraction of steam in the flow, i.e. the quality of the mixture, and let h_s and h_w denote the specific enthalpies of saturated steam and water. The specific internal energy of the mixture of steam and water is

$$h = \alpha_m h_s + (1 - \alpha_m)h_w = h_w + \alpha_m h_c. \tag{9}$$

In steady state we get

$$\frac{\partial q}{\partial z} = 0,$$

$$\frac{\partial qh}{\partial z} = qh_c\frac{\partial \alpha_m}{\partial z} = \frac{QA}{V}$$

and it then follows from Eq. (9) that

$$\alpha_m = \frac{QA}{qh_c V}z.$$

Let ξ be a normalized length coordinate along the risers and let α_r be the steam quality at the riser outlet. The steam fraction along the tube is

$$\alpha_m(\xi) = \alpha_r \xi, \quad 0 \le \xi \le 1. \tag{10}$$

A slight refinement of the model is to assume that boiling starts at a distance x_0 from the bottom of the risers. In this case the steam distribution will be characterized by two variables α_r and x_0 instead of just α_r. For the experimental data in this paper it adds very little to the prediction power of the model. For this reason we use the simpler model although the modification may be important for other boilers. There is actually a slip between water and steam in the risers. To take this into account requires much more complicated models. The justification for neglecting this is that it does not have a major influence on the fit to experimental data.

The volume and mass fractions of steam are related through $\alpha_v = f(\alpha_m)$, where

$$f(\alpha_m) = \frac{\varrho_w \alpha_m}{\varrho_s + (\varrho_w - \varrho_s)\alpha_m}. \tag{11}$$

It has been verified that the simple model which uses a linear steam-mass fraction given by Eq. (10) and a steam-volume fraction given by Eq. (11) describes quite well what happens in a typical riser tube. This is illustrated in Fig. 2 which compares the steam distribution in a tube computed from Eqs. (10) and (11) with computations from a detailed computational fluid dynamics code for a riser tube in a nuclear reactor. The complex code also takes into account that there is a slip between the flow of steam and water. It is interesting to see that the simple model captures the steam distribution quite well.

3.2. Average steam volume ratio

To model drum level it is essential to describe the total amount of steam in the risers. This is governed by the

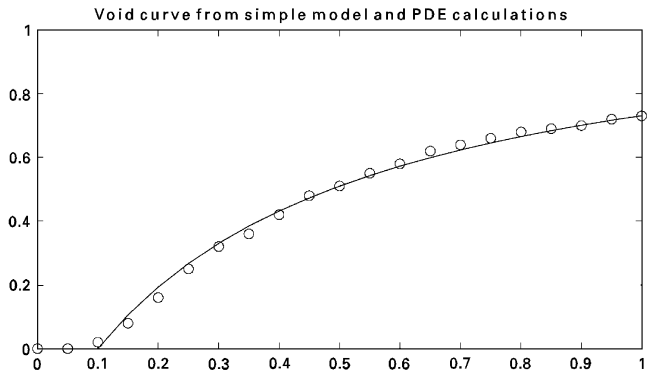

Fig. 2. Comparison of steady-state steam volume distribution calculated from Eqs. (10) and (11) (full lines) with results of numerical solutions of detailed partial differential equation models (circles).

average volume fraction in the risers. Assume that the mass fraction is linear along the riser as expressed by Eq. (10) we find that the average volume fraction $\bar{\alpha}_v$ is given by

$$\bar{\alpha}_v = \int_0^1 \alpha_v(\xi) = \frac{1}{\alpha_r}\int_0^{\alpha_r} f(\xi)\,d\xi = \frac{\varrho_w}{\varrho_w - \varrho_s} \times\left(1 - \frac{\varrho_s}{(\varrho_w - \varrho_s)\alpha_r}\ln\left(1 + \frac{\varrho_w - \varrho_s}{\varrho_s}\alpha_r\right)\right). \tag{12}$$

3.3. A lumped parameter model

Since we do not want to use partial differential equations they will be approximated using the Galerkin method. To do this it will be assumed that the steam-mass quality distribution is linear, i.e. Eq. (10) holds, also under dynamic conditions.

The transfer of mass and energy between steam and water by condensation and evaporation is a key element in the modeling. When modeling the phases separately the transfer must be accounted for explicitly. This can be avoided by writing joint balance equations for water and steam. The global mass balance for the riser section is

$$\frac{d}{dt}(\varrho_s\bar{\alpha}_v V_r + \varrho_w(1-\bar{\alpha}_v)V_r) = q_{dc} - q_r, \tag{13}$$

where q_r is the total mass flow rate out of the risers and q_{dc} is the total mass flow rate into the risers. The global energy balance for the riser section is

$$\frac{d}{dt}(\varrho_s h_s\bar{\alpha}_v V_r + \varrho_w h_w(1-\bar{\alpha}_v)V_r - pV_r + m_r C_p t_s) = Q + q_{dc}h_w - (\alpha_r h_c + h_w)q_r. \tag{14}$$

3.4. Circulation flow

For a forced circulation boiler downcomer flow rate, q_{dc} is a control variable. For a natural circulation boiler the flow rate is instead driven by the density gradients in the risers and the downcomers. The momentum balance for the downcomer riser loop is

$$(L_r + L_{dc})\frac{dq_{dc}}{dt} = (\varrho_w - \varrho_s)\bar{\alpha}_v V_r g - \frac{k}{2}\frac{q_{dc}^2}{\varrho_w A_{dc}},$$

where k is a dimensionless friction coefficient, L_r and L_{dc} are lengths and A_{dc} is the area. This is a first-order system with the time constant

$$T = \frac{(L_r + L_{dc})A_{dc}\varrho_w}{kq_{dc}}.$$

With typical numerical values we find that the time constant is about a second. This is short in comparison with the sampling period of our experimental data which is 10 s and we will therefore use the steady-state relation

$$\tfrac{1}{2}kq_{dc}^2 = \varrho_w A_{dc}(\varrho_w - \varrho_s)g\bar{\alpha}_v V_r. \tag{15}$$

3.5. Distribution of steam in the drum

The physical phenomena in the drum are complicated. Steam enters from many riser tubes, feedwater enters through a complex arrangement, water leaves through the downcomer tubes and steam through the steam valve. Geometry and flow patterns are complex. The basic mechanisms are separation of water and steam and condensation.

Let V_{sd} and V_{wd} be the volume of steam and water under the liquid level and let the steam flow rate through the liquid surface in the drum be q_{sd}. Recall that q_r is the flow rate out of the risers, q_f the feedwater flow rate and q_{dc} the downcomer flow rate. The mass balance for the steam under the liquid level is

$$\frac{d}{dt}(\varrho_s V_{sd}) = \alpha_r q_r - q_{sd} - q_{cd}, \tag{16}$$

where q_{cd} is the condensation flow which is given by

$$q_{cd} = \frac{h_w - h_f}{h_c}q_f + \frac{1}{h_c}\left(\varrho_s V_{sd}\frac{dh_s}{dt} + \varrho_w V_{wd}\frac{dh_w}{dt} - (V_{sd} + V_{wd})\frac{dp}{dt} + m_d C_p\frac{dt_s}{dt}\right). \tag{17}$$

The flow q_{sd} is driven by the density differences of water and steam, and the momentum of the flow entering the drum. Several models of different complexity have been attempted. Good fit to the experimental data have been obtained with the following empirical model:

$$q_{sd} = \frac{\varrho_s}{T_d}(V_{sd} - V_{sd}^0) + \alpha_r q_{dc} + \alpha_r\beta(q_{dc} - q_r). \tag{18}$$

Here V_{sd}^0 denotes the volume of steam in the drum in the hypothetical situation when there is no condensation of steam in the drum and T_d is the residence time of the steam in the drum.

3.6. Drum level

Having accounted for the distribution of the steam below the drum level, we can now model the drum level. The volume of water in the drum is

$$V_{\mathrm{wd}} = V_{\mathrm{wt}} - V_{\mathrm{dc}} - (1 - \bar{\alpha}_{\mathrm{v}})V_{\mathrm{r}}. \tag{19}$$

The drum has a complicated geometry. The linearized behavior can be described by the wet surface A_{d} at the operating level. The deviation of the drum level ℓ measured from its normal operating level is

$$\ell = \frac{V_{\mathrm{wd}} + V_{\mathrm{sd}}}{A_{\mathrm{d}}} = \ell_{\mathrm{w}} + \ell_{\mathrm{s}}. \tag{20}$$

The term ℓ_{w} represents level variations caused by changes of the amount of water in the drum and the term ℓ_{s} represents variations caused by the steam in the drum.

4. The model

Combining the results of Sections 2 and 3 we can now obtain a model that gives a good description of the boiler including the drum level. The model is given by the differential equations (1), (3), (13), (14), and (16). In addition there are a number of algebraic equations. The circulation flow rate q_{dc} is given by the static momentum balance (15), the steam flow rate through the liquid surface of the drum q_{sd} by (18), and the drum level ℓ by Eq. (20). The volumes are related through Eqs. (4) and (19). The model is a differential algebraic system, see Hairer, Lubich and Roche (1989). Since most available simulation software requires state equations we will also derive a state model.

4.1. Selection of state variables

State variables can be chosen in many different ways. It is convenient to choose states as variables with good physical interpretation that describe storage of mass, energy, and momentum. The accumulation of water is represented by the total water volume V_{wt}. The total energy is represented by the drum pressure p and the distribution of steam and water is captured by the steam-mass fraction in the risers α_{r} and the steam volume in the drum V_{sd}.

4.2. Pressure and water dynamics

State equations for pressure p and the total amount of water V_{wt} in the systems were obtained from the global mass and energy balances, Eqs. (1) and (3). These equations can be written as (5).

4.3. Riser dynamics

The mass and energy balances for the risers are given by Eqs. (13) and (14). Eliminating the flow rate out of the risers, q_{r}, by multiplying Eq. (13) by $-(h_{\mathrm{w}} + \alpha_{\mathrm{r}}h_{\mathrm{c}})$ and adding to Eq. (14) gives,

$$\begin{aligned}
&\frac{\mathrm{d}}{\mathrm{d}t}(\varrho_{\mathrm{s}}h_{\mathrm{s}}\bar{\alpha}_{\mathrm{v}}V_{\mathrm{r}}) - (h_{\mathrm{w}} + \alpha_{\mathrm{r}}h_{\mathrm{c}})\frac{\mathrm{d}}{\mathrm{d}t}(\varrho_{\mathrm{s}}\bar{\alpha}_{\mathrm{v}}V_{\mathrm{r}}) \\
&\quad + \frac{\mathrm{d}}{\mathrm{d}t}(\varrho_{\mathrm{w}}h_{\mathrm{w}}(1 - \bar{\alpha}_{\mathrm{v}})V_{\mathrm{r}}) \\
&\quad - (h_{\mathrm{w}} + \alpha_{\mathrm{r}}h_{\mathrm{c}})\frac{\mathrm{d}}{\mathrm{d}t}(\varrho_{\mathrm{w}}(1 - \bar{\alpha}_{\mathrm{v}})V_{\mathrm{r}}) \\
&\quad - V_{\mathrm{r}}\frac{\mathrm{d}p}{\mathrm{d}t} + m_{\mathrm{r}}C_p\frac{\mathrm{d}t_{\mathrm{s}}}{\mathrm{d}t} = Q - \alpha_{\mathrm{r}}h_{\mathrm{c}}q_{\mathrm{dc}}.
\end{aligned}$$

This can be simplified to

$$\begin{aligned}
&h_{\mathrm{c}}(1 - \alpha_{\mathrm{r}})\frac{\mathrm{d}}{\mathrm{d}t}(\varrho_{\mathrm{s}}\bar{\alpha}_{\mathrm{v}}V_{\mathrm{r}}) + \varrho_{\mathrm{w}}(1 - \bar{\alpha}_{\mathrm{v}})V_{\mathrm{r}}\frac{\mathrm{d}h_{\mathrm{w}}}{\mathrm{d}t} \\
&\quad - \alpha_{\mathrm{r}}h_{\mathrm{c}}\frac{\mathrm{d}}{\mathrm{d}t}(\varrho_{\mathrm{w}}(1 - \bar{\alpha}_{\mathrm{v}})V_{\mathrm{r}}) + \varrho_{\mathrm{s}}\bar{\alpha}_{\mathrm{v}}V_{\mathrm{r}}\frac{\mathrm{d}h_{\mathrm{s}}}{\mathrm{d}t} \\
&\quad - V_{\mathrm{r}}\frac{\mathrm{d}p}{\mathrm{d}t} + m_{\mathrm{r}}C_p\frac{\mathrm{d}t_{\mathrm{s}}}{\mathrm{d}t} = Q - \alpha_{\mathrm{r}}h_{\mathrm{c}}q_{\mathrm{dc}}.
\end{aligned} \tag{21}$$

If the state variables p and α_{r} are known the riser flow rate q_{r} can be computed from Eq. (13). This gives

$$\begin{aligned}
q_{\mathrm{r}} &= q_{\mathrm{dc}} - \frac{\mathrm{d}}{\mathrm{d}t}(\varrho_{\mathrm{s}}\bar{\alpha}_{\mathrm{v}}V_{\mathrm{r}}) - \frac{\mathrm{d}}{\mathrm{d}t}(\varrho_{\mathrm{w}}(1 - \bar{\alpha}_{\mathrm{v}})V_{\mathrm{r}}) \\
&= q_{\mathrm{dc}} - V_{\mathrm{r}}\frac{\mathrm{d}}{\mathrm{d}t}((1 - \bar{\alpha}_{\mathrm{v}})\varrho_{\mathrm{w}} + \bar{\alpha}_{\mathrm{v}}\varrho_{\mathrm{s}}) \\
&= q_{\mathrm{dc}} - V_{\mathrm{r}}\frac{\mathrm{d}}{\mathrm{d}t}(\varrho_{\mathrm{w}} - \bar{\alpha}_{\mathrm{v}}(\varrho_{\mathrm{w}} - \varrho_{\mathrm{s}})) \\
&= q_{\mathrm{dc}} - V_{\mathrm{r}}\frac{\partial}{\partial p}((1 - \bar{\alpha}_{\mathrm{v}})\varrho_{\mathrm{w}} + \bar{\alpha}_{\mathrm{v}}\varrho_{\mathrm{s}})\frac{\mathrm{d}p}{\mathrm{d}t} \\
&\quad + V_{\mathrm{r}}(\varrho_{\mathrm{w}} - \varrho_{\mathrm{s}})\frac{\partial\bar{\alpha}_{\mathrm{v}}}{\partial\alpha_{\mathrm{r}}}\frac{\mathrm{d}\alpha_{\mathrm{r}}}{\mathrm{d}t}.
\end{aligned} \tag{22}$$

4.4. Drum dynamics

The dynamics for the steam in the drum is obtained from the mass balance (16). Introducing expression (22) for q_{r}, expression (17) for q_{cd} and expression (18) for

q_{sd} into this equation we find

$$\varrho_s \frac{dV_{sd}}{dt} + V_{sd}\frac{d\varrho_s}{dt} + \frac{1}{h_c}\left(\varrho_s V_{sd}\frac{dh_s}{dt} + \varrho_w V_{wd}\frac{dh_w}{dt} - (V_{sd} + V_{wd})\frac{dp}{dt} + m_d C_p \frac{dt_s}{dt}\right) + \alpha_r(1+\beta)V_r \frac{d}{dt}((1-\bar{\alpha}_v)\varrho_w + \bar{\alpha}_v \varrho_s) = \frac{\varrho_s}{T_d}(V_{sd}^0 - V_{sd}) + \frac{h_f - h_w}{h_c} q_f. \tag{23}$$

Many of the complex phenomena in the drum are captured by this equation.

4.5. Summary

The state variables are: drum pressure p, total water volume V_{wt}, steam quality at the riser outlet α_r, and volume of steam under the liquid level in the drum V_{sd}. The time derivatives of these variables are given by Eqs. (5), (21), and (23). Straightforward but tedious calculations show that these equations can be written as

$$\begin{aligned} e_{11}\frac{dV_{wt}}{dt} + e_{12}\frac{dp}{dt} &= q_f - q_s, \\ e_{21}\frac{dV_{wt}}{dt} + e_{22}\frac{dp}{dt} &= Q + q_f h_f - q_s h_s, \\ e_{32}\frac{dp}{dt} + e_{33}\frac{d\alpha_r}{dt} &= Q - \alpha_r h_c q_{dc}, \\ e_{42}\frac{dp}{dt} + e_{43}\frac{d\alpha_r}{dt} + e_{44}\frac{dV_{sd}}{dt} &= \frac{\varrho_s}{T_d}(V_{sd}^0 - V_{sd}) + \frac{h_f - h_w}{h_c} q_f, \end{aligned} \tag{24}$$

where $h_c = h_s - h_w$ and

$$\begin{aligned} e_{11} &= \varrho_w - \varrho_s, \\ e_{12} &= V_{wt}\frac{\partial \varrho_w}{\partial p} + V_{st}\frac{\partial \varrho_s}{\partial p}, \\ e_{21} &= \varrho_w h_w - \varrho_s h_s, \\ e_{22} &= V_{wt}\left(h_w \frac{\partial \varrho_w}{\partial p} + \varrho_w \frac{\partial h_w}{\partial p}\right) + V_{st}\left(h_s \frac{\partial \varrho_s}{\partial p} + \varrho_s \frac{\partial h_s}{\partial p}\right) - V_t + m_t C_p \frac{\partial t_s}{\partial p}, \\ e_{32} &= \left(\varrho_w \frac{\partial h_w}{\partial p} - \alpha_r h_c \frac{\partial \varrho_w}{\partial p}\right)(1-\bar{\alpha}_v)V_r + \left((1-\alpha_r)h_c \frac{\partial \varrho_s}{\partial p} + \varrho_s \frac{\partial h_s}{\partial p}\right)\bar{\alpha}_v V_r \\ &\quad + (\varrho_s + (\varrho_w - \varrho_s)\alpha_r)\, h_c V_r \frac{\partial \bar{\alpha}_v}{\partial p} - V_r + m_r C_p \frac{\partial t_s}{\partial p}, \\ e_{33} &= ((1-\alpha_r)\varrho_s + \alpha_r \varrho_w) h_c V_r \frac{\partial \bar{\alpha}_v}{\partial \alpha_r} \\ e_{42} &= V_{sd}\frac{\partial \varrho_s}{\partial p} + \frac{1}{h_c}\left(\varrho_s V_{sd}\frac{\partial h_s}{\partial p} + \varrho_w V_{wd}\frac{\partial h_w}{\partial p} - V_{sd} - V_{wd} + m_d C_p \frac{\partial t_s}{\partial p}\right) + \alpha_r(1+\beta)V_r \left(\bar{\alpha}_v \frac{\partial \varrho_s}{\partial p} + (1-\bar{\alpha}_v)\frac{\partial \varrho_w}{\partial p} + (\varrho_s - \varrho_w)\frac{\partial \bar{\alpha}_v}{\partial p}\right), \\ e_{43} &= \alpha_r(1+\beta)(\rho_s - \rho_w)V_r \frac{\partial \bar{\alpha}_v}{\partial \alpha_r}, \\ e_{44} &= \varrho_s. \end{aligned} \tag{25}$$

In addition steam tables are required to evaluate $h_s, h_w, \rho_s, \rho_w, \partial\rho_s/\partial p, \partial\rho_w/\partial p, \partial h_s/\partial p, \partial h_w/\partial p, t_s$, and $\partial t_s/\partial p$ at the saturation pressure p. The results in Sections 5 and 6 are based on approximations of steam tables with quadratic functions. More elaborated approximations with table look-up and interpolation have been tried but the differences in the dynamic responses are not significant.

The steam volume fraction $\bar{\alpha}_v$ is given by Eq. (12), the volume of water in drum V_{wd} by Eq. (19), the drum level ℓ by Eq. (20), and the downcomer mass flow rate q_{dc} by Eq. (15).

The partial derivatives of the steam volume fraction with respect to pressure and mass fraction are obtained by differentiating Eq. (12). We get

$$\begin{aligned} \frac{\partial \bar{\alpha}_v}{\partial p} &= \frac{1}{(\rho_w - \rho_s)^2}\left(\rho_w \frac{\partial \rho_s}{\partial p} - \rho_s \frac{\partial \rho_w}{\partial p}\right)\left(1 + \frac{\rho_w}{\rho_s}\frac{1}{1+\eta} - \frac{\rho_s + \rho_w}{\eta \rho_s}\ln(1+\eta)\right) \\ \frac{\partial \bar{\alpha}_v}{\partial \alpha_r} &= \frac{\varrho_w}{\varrho_s \eta}\left(\frac{1}{\eta}\ell n(1+\eta) - \frac{1}{1+\eta}\right), \end{aligned} \tag{26}$$

where $\eta = \alpha_r(\varrho_w - \varrho_s)/\varrho_s$.

It is also of interest to know the total condensation flow rate q_{ct} and the flow rate out of the risers q_r. These flows are given by Eqs. (8) and (22), hence

$$\bar{\alpha}_v = \frac{\varrho_w}{\varrho_w - \varrho_s}\left(1 - \frac{\varrho_s}{(\varrho_w - \varrho_s)\alpha_r}\ln\left(1 + \frac{\varrho_w - \varrho_s}{\varrho_s}\alpha_r\right)\right),$$

$$V_{wd} = V_{wt} - V_{dc} - (1 - \bar{\alpha}_v)V_r,$$

$$\ell = \frac{V_{wd} + V_{sd}}{A_d},$$

$$T_d = \frac{\rho_s V_{sd}^0}{q_{sd}},$$

$$q_{dc}^2 = \frac{2\varrho_w A_{dc}(\varrho_w - \varrho_s)g\bar{\alpha}_v V_r}{k}$$

$$q_{ct} = \frac{h_w - h_f}{h_c}q_f + \frac{1}{h_c}\left(\varrho_s V_{st}\frac{\partial h_s}{\partial p} + \varrho_w V_{wt}\frac{\partial h_w}{\partial p} - V_t + m_t C_p \frac{\partial t_s}{\partial p}\right)\frac{dp}{dt},$$

$$q_r = q_{dc} - V_r\left(\bar{\alpha}_v\frac{\partial \varrho_s}{\partial p} + (1 - \bar{\alpha}_v)\frac{\partial \varrho_w}{\partial p} + (\rho_w - \rho_s)\frac{\partial \bar{\alpha}_v}{\partial p}\right)\frac{dp}{dt} + (\rho_w - \rho_s)V_r\frac{\partial \bar{\alpha}_v}{\partial \alpha_r}\frac{d\alpha_r}{dt}.$$

4.6. Structure of the equations

Note that Eq. (24) has an interesting lower triangular structure where the state variables can be grouped as $(((V_{wt}, p), \alpha_r), V_{sd})$ where the variables inside each parenthesis can be computed independently. The model can thus be regarded as a nesting of a second-, a third-, and a fourth-order model. The second-order model describes drum pressure and total volume of water in the system. The equations are global mass and energy balances. There is a very weak coupling between these equations which is caused by the condensation flow. The third-order model captures the steam dynamics in the risers and the fourth-order model also describes the dynamics of steam below the water surface in the drum. The third equation is a combination of mass and energy balances for the riser, and the fourth equation is a mass balance for steam under the water level in the drum.

Linearizing Eq. (24) shows that the system has a double pole at the origin and poles at $-h_c q_{dc}/e_{33}$ and $-1/T_d$. One pole at the origin is associated with water dynamics and the other with pressure dynamics. The pole associated with pressure dynamics is at the origin because the steam flow is chosen as a control variable. The pole moves into the left half-plane when the drum is connected to the turbines. The poles $-h_c q_{dc}/e_{33}$ and $-1/T_d$ are associated with dynamics of steam in the risers and the drum.

The nested structure reflects how the model was developed. The third-order model is an improved version of the models in Åström and Bell (1988). In Bell and Åström (1996) we added drum dynamics as a fourth-order model. The model in this paper is a refined version of that model. Different models of higher order have also been developed.

4.7. Parameters

An interesting feature of the model is that it requires only nine parameters:

- drum volume V_d,
- riser volume V_r,
- downcomer volume V_{dc},
- drum area A_d at normal operating level,
- total metal mass m_t,
- total riser mass m_r,
- friction coefficient in downcomer-riser loop k,
- residence time T_d of steam in drum,
- parameter β in the empirical equation (18).

A convenient way to find the parameter k is to compute it from the circulation flow rate. Perturbation studies have shown that the behavior of the system is not very sensitive to the parameters.

The parameters used in this paper were based on construction data. Some of them were quite crude. Gray-box identification, Bohlin (1991) was used in a comprehensive investigation in Eborn and Sørlie (1997) and Sørlie and Eborn (1999). Parameters were estimated and hypothesis testing was used to compare several model structures. The results showed that pressure dynamics can be improved significantly by increasing the metal masses. Significant improvements can also be obtained by adjusting the coefficients in the calibration formula for the sensors.

In Sørlie and Eborn (1999) it was shown that the friction coefficient is not identifiable from the data. There is in fact a relation between the initial steam quality and friction. A consequence of this is that it is highly desirable for accurate modeling to measure the circulation flow. This could also be an important signal to use in a level control system.

In Eborn and Sørlie (1997) hypothesis testing was applied to the models Åström and Bell (1988, 1993) (third order) and Bell and Åström (1996) (fourth order). These studies showed conclusively that the improvements obtained with the fourth-order model are significant. Computations on fifth-order models with a more detailed representation of the drum showed that the increased complexity could not be justified.

4.8. Equilibrium values

The steady-state solution of Eq. (24) is given by

$$q_f = q_s,$$

$$Q = q_s h_s - q_f h_f,$$

$$Q = q_{dc}\alpha_r h_c,$$

$$V_{sd} = V_{sd}^0 - \frac{T_d(h_w - h_f)}{\varrho_s h_c}q_f,$$

where q_{dc} is given by Eq. (15), i.e.

$$q_{dc} = \sqrt{\frac{2\varrho_w A_{dc}(\varrho_w - \varrho_s) g \bar{\alpha}_v V_r}{k}}.$$

A convenient way to find the initial values is to first specify steam flow rate q_s and steam pressure p. The feedwater flow rate q_f and the input power Q are then given by the first two equations and the steam volume in the drum is given by the last equation. The steam quality α_r is obtained by solving the nonlinear equations

$$Q = \alpha_r h_c \sqrt{\frac{2\varrho_w A_{dc}(\varrho_w - \varrho_s) g \bar{\alpha}_v V_r}{k}}$$

$$\bar{\alpha}_v = \frac{\varrho_w}{\varrho_w - \varrho_s}\left(1 - \frac{\varrho_s}{(\varrho_w - \varrho_s)\alpha_r} \ln\left(1 + \frac{\varrho_w - \varrho_s}{\varrho_s}\alpha_r\right)\right). \tag{27}$$

The steam volume in the drum can then be computed directly.

Eq. (27) defines the steam volume ratio $\bar{\alpha}_v$ as a function of the input power Q. This function which is shown in Fig. 3 gives important insight into the shrink and swell phenomena. The curve shows that a given change in input power gives a larger variation in average steam volume ratio at low power. This explains why the shrink and swell effects are larger at low power than at high power.

4.9. Impact of modeling languages

Development of physical models is a tedious iterative process. Different physical assumptions are made, a model is developed and compared with experiments by simulation, parameters may be fitted. Detailed investigation of the results gives ideas for improvements and modifications. It is a significant effort to transform the equations to state space form because of the algebra involved. This is reflected in the manipulations resulting in Eq. (24). Many intermediate steps have actually been omitted in the paper. The modeling effort can be reduced substantially by using modeling languages such as Dymola, Elmqvist (1978), Omola, Mattsson et al. (1993), or Modelica, Elmqvist, Mattsson and Otter (1998). In these languages the model is described in its most basic form in terms of differential algebraic equations. In our case this means that the basic mass and energy balances, such as (1) and (2), are entered into the system together with the algebraic equations, such as (4). The software then makes algebraic manipulations symbolically to simplify the equations for efficient simulation.

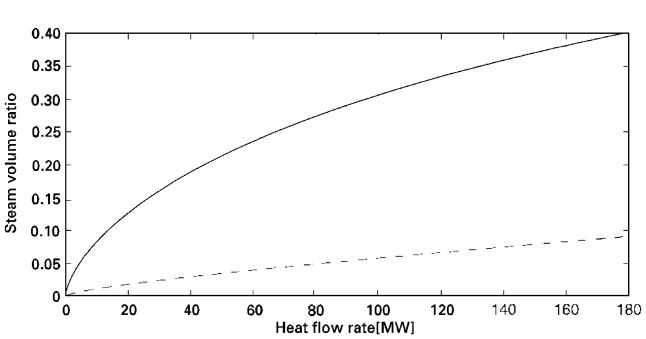

Fig. 3. Steady-state relation between steam volume ratio $\bar{\alpha}_v$ and input power Q. The dashed curve shows the steam mass ratio α_r.

5. Step responses

To illustrate the dynamic behavior of the model we will simulate responses to step changes in the inputs. Since there are many inputs and many interesting variables we will focus on a few selected responses. One input was changed and the others were kept constant. The magnitudes of the changes were about 10% of the nominal values of the signals. To compare responses at different load conditions the same amplitudes were used at high and medium load.

5.1. Plant parameters

The parameters used were those from the Swedish power plant. The values are $V_d = 40\,\mathrm{m}^3$, $V_r = 37\,\mathrm{m}^3$, $V_{dc} = 11\,\mathrm{m}^3$, $A_d = 20\,\mathrm{m}^2$, $m_t = 300{,}000\,\mathrm{kg}$, $m_r = 160{,}000\,\mathrm{kg}$, $k = 25, \beta = 0.3$, and $T_d = 12\,\mathrm{s}$. The steam tables were approximated by quadratic functions.

5.2. Fuel flow changes at medium load

Fig. 4 shows the responses of the state variables, the circulation flow rate q_{dc}, the riser flow rate q_r, and the total condensation flow rate q_{ct} to a step increase in fuel flow rate equivalent to 10 MW. Pressure increases at approximately constant rate. The reason for this is that steam flow out of the drum is constant. Total water volume V_{wt} increases due to the condensation that occurs due to the increasing pressure. Steam quality at the riser outlet α_r first increases rapidly and then more gradually. The volume of steam in the drum first increases a little and it then decreases. The rapid initial increase in steam volume is due to the fast increase in steam from the risers. The decrease is due to the increased pressure which causes condensation of the steam. At the onset of the step there is a rapid increase in the outlet flow rate from the risers. The flow then decreases to match the downcomer flow rate. The flow rates are equal after about 30 s. The condensation flow changes in a step-like manner.

5.3. Steam flow changes at medium load

Fig. 5 shows the responses to a step increase of 10 kg/s in steam flow rate at medium load. Pressure decreases

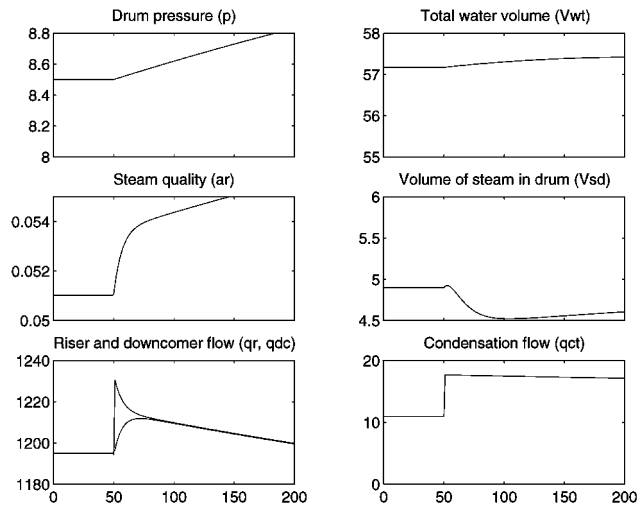

Fig. 4. Responses to a step in fuel flow rate of 10 MW at medium load.

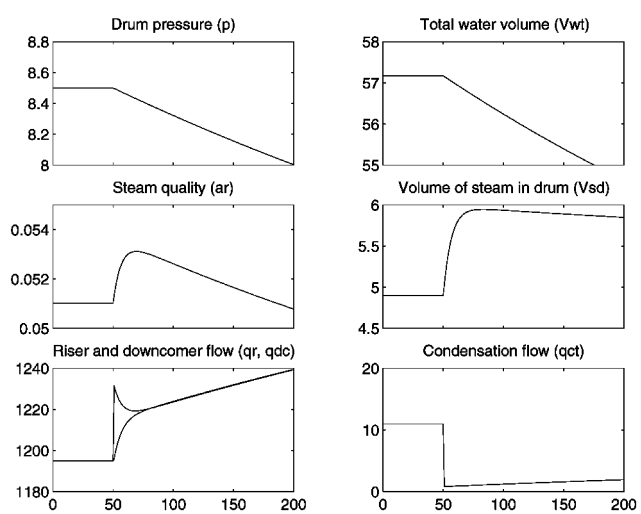

Fig. 5. Responses to a step in steam flow rate of 10 kg/s at medium load.

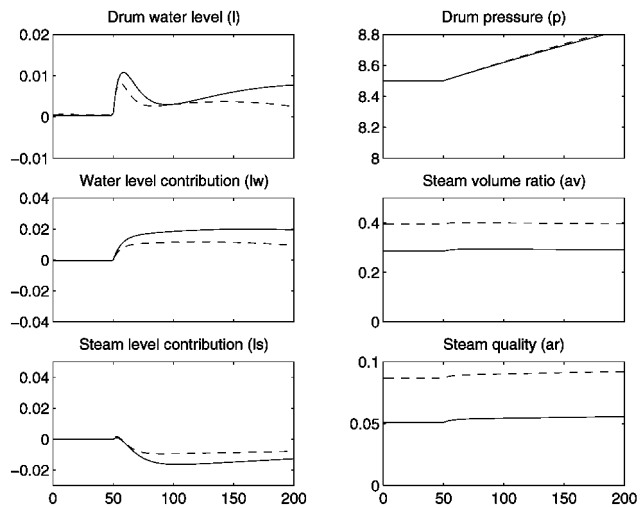

Fig. 6. Responses to a step in fuel flow rate of 10 MW at medium (solid) and high (dashed) loads.

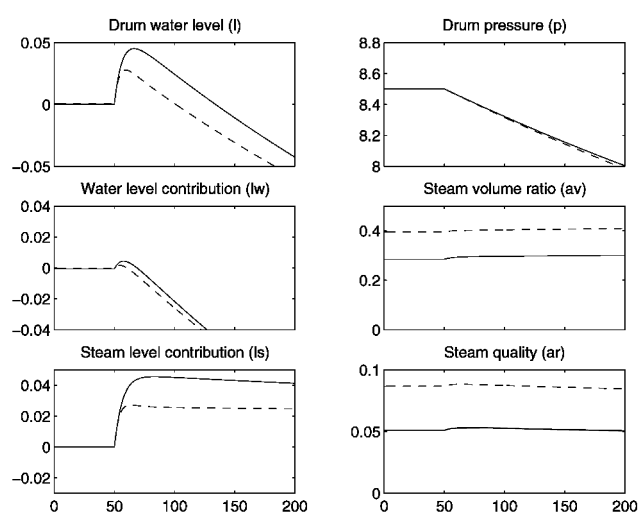

Fig. 7. Responses to a step in steam flow rate of 10 kg/s at medium (solid) and high (dashed) loads.

practically linearly because of the increased steam flow. Total water volume also decreases because of increased evaporation due to the decreasing pressure. Steam quality at the riser outlet first increases rapidly due to the pressure decrease and it then decreases due to the increased circulation flow rate. The volume of the steam in the drum increases due to the decreased pressure. There is a very rapid increase of flow out of the riser due to the pressure drop. After this initial transient the riser flow rate then decreases to match the downcomer flow rate. There is a steady increase in both due to the decreased pressure. The condensation flow drops in an almost step-like fashion because the pressure decreases at constant rate.

5.4. Drum level responses

Since the behavior of the drum level is of particular interest we will show step responses that give good insight into drum level dynamics for different operating conditions. It follows from Eq. (20) that drum level is the sum of $\ell_w = V_{wd}/A_d$ and $\ell_s = V_{sd}/A_d$, which depend on the volumes of water and steam in the drum. Drum pressure, steam mass, and volume fractions will also be shown. Responses for medium and high load will be given to illustrate the dependence on operating conditions.

Fig. 6 shows the response to a step in fuel flow corresponding to 10 MW. The response in drum level is complicated and depends on a combination of the dynamics

of water and steam in the drum. The initial part of the swell is due to the rapid initial response of steam that was also seen in Fig. 4. The response in level is a combination of two competing mechanisms. The water volume in the drum increases due to increased condensation caused by the increasing pressure. The volume of the steam in the drum first increases a little and it then decreases because of the increasing pressure. Note that there are significant changes in steam quality and steam volume ratio for the different operating conditions. Compare with Fig. 3.

Fig. 7 shows the response to a step increase in steam flow rate of 10 kg/s. There is a strong shrink and swell effect in this case too. The contributions from the volumes of steam and water have the same sign initially. The water volume will, however, decrease because of the steam flow.

6. Comparisons with plant data

Much of the model development was based on plant experiments performed with the P16-G16 unit at Öresundsverket in Malmö, Sweden in collaboration with Sydkraft AB. The experiments are described in Eklund (1971) and Åström and Eklund (1972, 1975). They were carried out in open loop with the normal regulators removed. The signals were filtered and sampled at a rate of 0.1 Hz. To ensure a good excitation of the process PRBS-like perturbations were introduced in fuel flow rate, feedwater flow rate, and steam flow rate. The intention was to change one input signal in each experiment. To ensure that critical variables such as drum water level did not go outside safe limit we made manual correction occasionally. This means that several inputs were changed in each experiment. The steam flow rate changed in response to pressure changes in all experiments because we were unable to control it tightly.

A large number of signals were logged during the experiment. This proved to be very valuable because it has been possible to use the data for a very large number of investigations. The experiments were performed both at high and medium load. In this paper we have used data where three variables, fuel flow rate, feedwater flow rate, and steam flow rate were changed. This gives a total of six experiments which can be used to validate the model.

There were problems with the calibration of the flow rate measurement transducers and also some uncertainty in the effective energy content of the oil. The approach used was to start with the nominal calibration values and then make small corrections so that the long-term tracking between the plant data and the model was as close as possible. The change in all cases was well within the transducers accuracy limits. Apart from that, no fiddling with the coefficients was made. When showing the results in the following, we present the primary input variable and the responses in drum pressure and drum level.

6.1. Experiments at medium load

The results of experiments at medium load will be described first. This is the operating condition where the shrink and swell phenomenon is most pronounced.

6.1.1. Fuel flow rate changes

Fig. 8 shows responses in drum pressure and drum level for perturbations in fuel flow rate. There is very good agreement between the model and the experimental data for drum pressure and drum water level. Note in particular that there is an overshoot in the drum level response for step changes in fuel flow. This is caused by the interaction between the two state variables that describe the dynamics of steam under the liquid level in the drum.

6.1.2. Changes in feedwater flow rate

Fig. 9 shows the responses to changes in the feedwater flow rate. The general character of the responses agrees well. There are some deviations in the pressure responses and some of the finer details of the drum level are exaggerated. The pressure does deviate in the 500–1500 s region, but since the changes in pressure are small the results are considered adequate.

6.1.3. Changes in the steam valve

Fig. 10 shows the responses to changes in the steam valve. There is very good agreement between the model and the experimental data. Note that there is a significant shrink and swell effect which is captured very well by the model.

6.2. Experiments at high load

6.2.1. Changes in fuel flow rate

Fig. 11 shows responses in drum pressure and drum level for perturbations in fuel flow rate. There is good

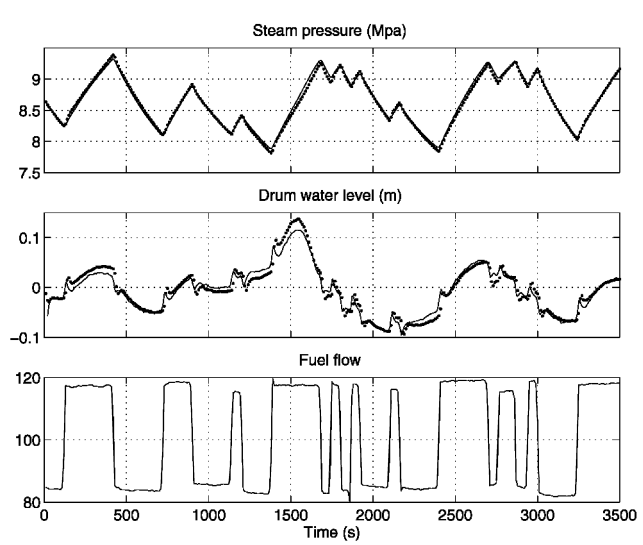

Fig. 8. Comparison of model (solid line) and plant data (dots) for perturbations in fuel flow rate at medium load.

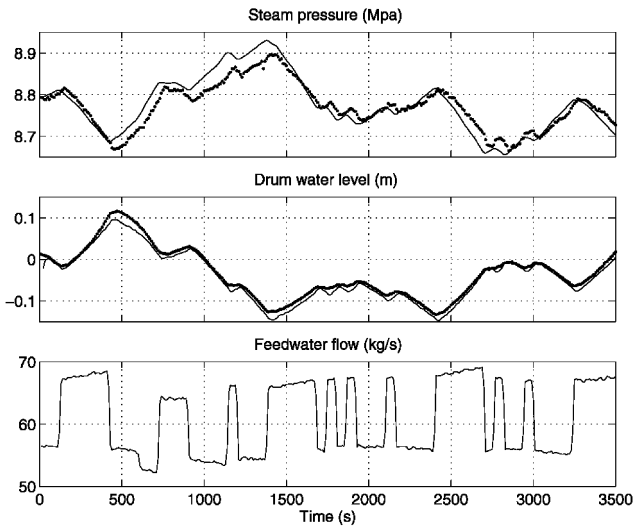

Fig. 9. Comparison of model (solid line) and plant data (dots) for perturbations in feedwater flow rate at medium load.

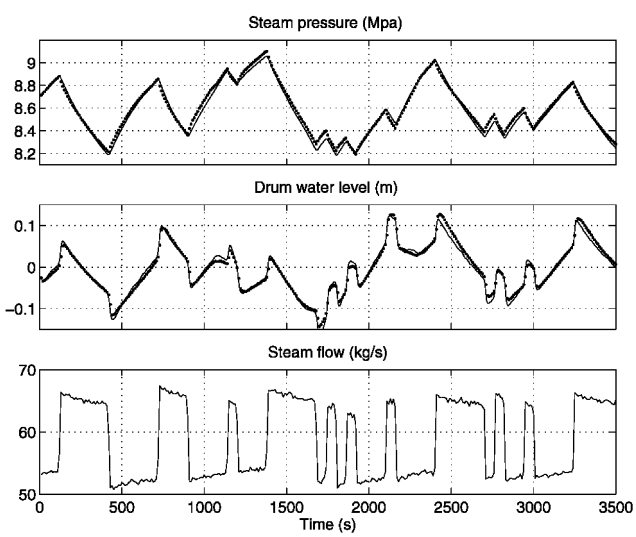

Fig. 10. Comparison of model (solid line) and plant data (dots) for perturbations in steam flow rate at medium load.

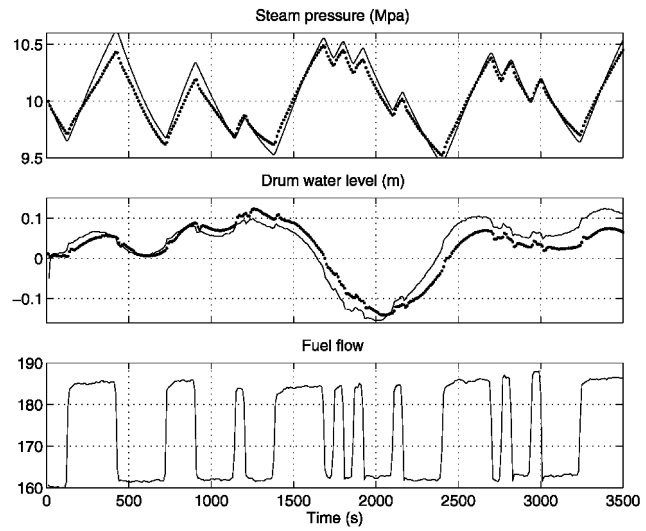

Fig. 11. Comparison of model (solid line) and plant data (dots) for perturbations in fuel flow rate at high load.

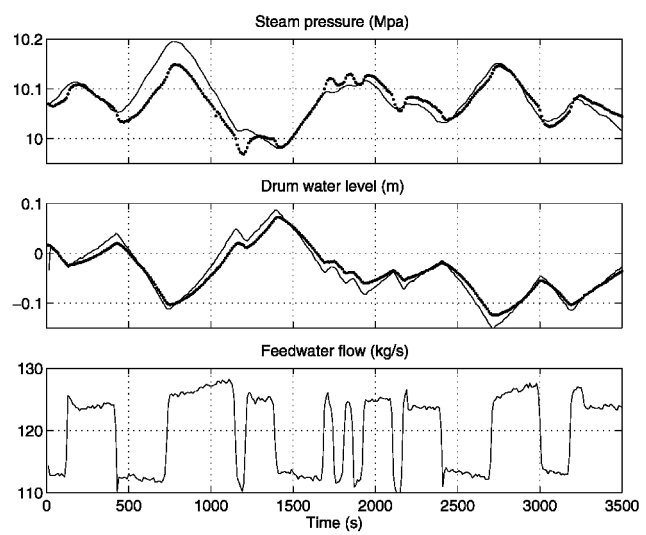

Fig. 12. Comparison of model (solid line) and plant data (dots) for perturbations in feedwater flow rate at high load.

agreement between the model and the experimental data. A comparison with Fig. 8 shows that the shrink and swell effect is much smaller at high load. It is interesting to see that the model captures this.

6.2.2. Changes in feedwater flow rate

Fig. 12 shows the responses to changes in feedwater flow rate. There are discrepancies in pressure from time 400 to 1400. The total changes in pressure are small and minor variations in feedwater conditions can easily cause variations of this magnitude. The model exaggerates the level changes for rapid variations. Compare for example data in the interval 1500–2000.

6.2.3. Changes in the steam valve

Fig. 13 shows the responses to changes in the steam flow rate. There is very good agreement between the model and the experimental data. Note that the model captures the drum level variations, particularly the swell and shrink effect very well. A comparison with Fig. 10 shows that the shrink and swell effect is smaller at high loads. This is well captured by the model.

6.3. Comparison of behavior at high and medium load

The experiments have indicated that there are significant differences in behavior at high and medium loads that are well predicted by the model. We will now look closer at these differences.

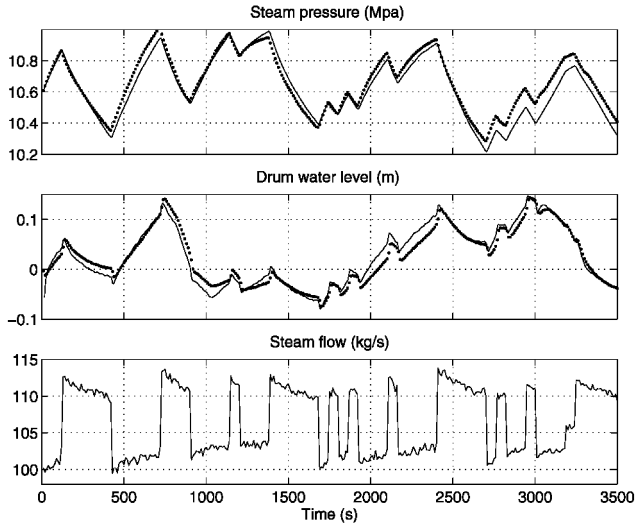

Fig. 13. Comparison of model (solid line) and plant data (dots) for perturbations in steam flow rate at high load.

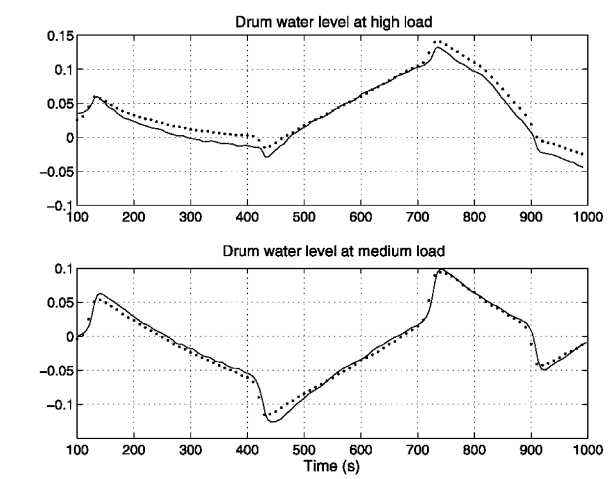

Fig. 14. Comparison of behavior of drum water level at medium and high loads for perturbations in steam flow rate. The model response is shown in solid lines and plant data is indicated by dots.

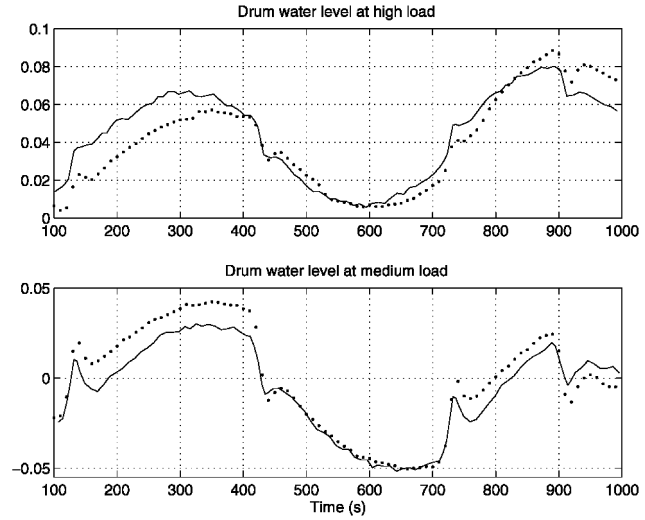

Fig. 15. Comparison of behavior of drum water level at medium and high loads for perturbations in fuel flow rate. The model response is shown in solid lines and plant data is indicated by dots.

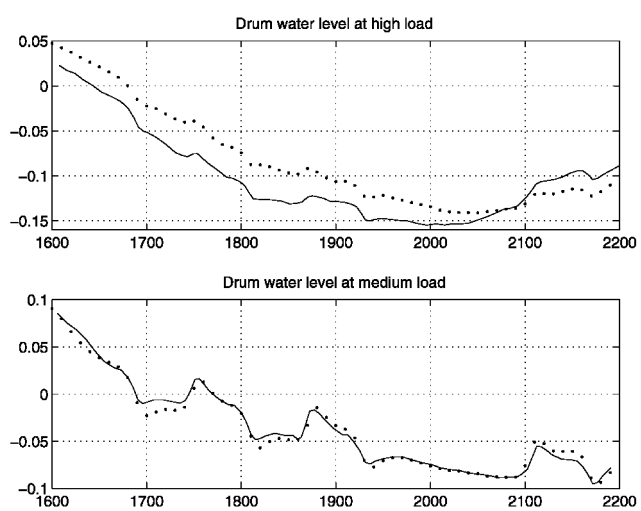

Fig. 16. Comparison of behavior of drum water level at medium and high loads for perturbations in fuel flow rate. The model response is shown in solid lines and plant data is indicated by dots.

Fig. 14 compares the responses in drum level to steam flow changes at high and medium loads. The steam valve changes were almost the same in both experiments (as is shown in Figs. 10 and 13) but they were not identical. Because of the integrators in the model there are natural differences in the levels of the signals. Apart from this level shift the model matches the experiments very well. Fig. 14 also shows that the shrink and swell effect is larger at medium load. It is even larger at low loads.

Fig. 15 compares responses to changes in fuel flow. Note the good agreement for dynamic responses between the model and experiments. In this case there is a pronounced difference between the behaviors for medium and high load. Fig. 16 compares responses to changes in fuel flow. We have taken a section of the data where there are substantial rapid variations. Again we note the excellent agreement between model and experiments and we also note the significant difference between the behaviors at medium and high loads.

7. Conclusions

A nonlinear physical model with a complexity that is suitable for model-based control has been presented. The model is based on physical parameters for the plant and can be easily scaled to represent any drum power station. The model has four states; two account for storage of total energy and total mass, one characterizes steam distribution in the risers and another the steam distribu-

tion in the drum. The model can be characterized by steam tables and a few physical parameters.

The model is nonlinear and agrees well with experimental data. In particular, the complex shrink and swell phenomena associated with the drum water level are well captured by the model. The model has a triangular structure that can be described as $(((V_{wt}, p), \alpha_r), V_{sd})$, where the states in each bracket can be determined sequentially. The linearized model has two poles at the origin and two real stable poles.

The model has been validated against plant data with very rich excitation that covers a wide operating range. These experiments have given much insight into the behavior of the system and they have guided the modeling effort. We believe that the approach used in this work can be applied to other configurations of steam generators.

Model (24) can be simplified by keeping only the dominant terms in expressions (25) for the coefficients e_{ij}. This could be useful for applications to model-based control. Preliminary investigations indicate that several terms can be neglected without sacrificing the fit to experimental data. A comprehensive study of this is outside the scope of this paper. The model can also be refined in several ways. This will, however, require new measurements with faster sampling rates.

Acknowledgements

The research has been supported by the Sydkraft Research Foundation and the Swedish National Board for Industrial and Technical Development under contract 97-04573. This support is gratefully acknowledged. We would also like to express our sincere gratitude to Sydkraft AB for their willingness to perform experiments on plants to increase our understanding of their behavior. Useful comments on several versions of the manuscript have been given by our colleagues J. Eborn, H. Tummescheit, and A. Glattfelder. We would also like to express our gratitude to the reviewers for constructive criticism.

References

Ambos, P., Duc, G., & Falinower, C.-M. (1996). Loop shaping H_∞ design applied to the steam generator level control in edf nuclear power plants. In *Proceedings of fifth IEEE conference on control applications* (pp. 751–756). Dearborn, Michigan: IEEE.

Åström, K. J. (1972). Modelling and identification of power system components. In Handschin, *Real-time control of electric power systems*, *Proceedings of Symposium on real-time control of electric power system*, Baden, Switzerland, 1971 (pp. 1–28). Amsterdam: Elsevier.

Åström, K. J., & Bell, R. (1988). Simple drum-boiler models. In *IFAC international symposium on power systems, modelling and control applications*. Brussels, Belgium.

Åström, K. J., & Bell, R. D. (1993). A nonlinear model for steam generation process. In *Preprints IFAC 12th world congress*. Sydney, Australia.

Åström, K. J., & Eklund, K. (1972). A simplified non-linear model for a drum boiler — Turbine unit. *International Journal of Control*, *16*, 145–169.

Åström, K. J., & Eklund, K. (1975). A simple non-linear drum-boiler model. *International Journal of Control*, *22*, 739–740.

Bell, R. D. (1973). *The on-line optimal control of constrained non-linear processes and its application to steam generators*. Ph.D. thesis, University of N.S.W., Australia.

Bell, R. D., & Åström, K. J. (1996). A fourth order non-linear model for drum-boiler dynamics. In *IFAC'96*, Preprints 13th World Congress of IFAC, vol. O, San Francisco, CA (pp. 31–36).

Bell, R. D., Rees, N.W., & Lee, K.B. (1977). Models of large boiler-turbine plant. In *IFAC symposium on automatic control & protection of electric power systems* (pp. 469–475). Ins. of Engineers, Aust. National Conf. Publ.

Bohlin, T. (1991). *Interactive system identification: Prospects and pitfalls*. Berlin: Springer.

Borsi, L. (1974). Extended linear mathematical model of a power station unit with a once through boiler. *Siemens Forschungs und Entwicklingsberichte*, *3*(5), 274–280.

Caseau, P., & Godin, P. (1969). Mathematical modelling of power plants. IE(Australia) Electronic Engineering Transactions.

Cheng, C. M., & Rees, N. W. (1997). Fuzzy model based control of steam generation in drum-boiler power plant. In *Proceedings of IFAC/CIGRE symposium on control of power systems and power plants CPSPP'97*, Beijing, China (pp. 175–181). International Academic Publishers.

Chien, K. L., Ergin, E. I., Ling, C., & Lee, A. (1958). Dynamic analysis of a boiler. *Transactions of ASME*, *80*, 1809–1819.

de Mello, F. P. (1963). Plant dynamics and control analysis. *IEEE Transactions on Power Apparatus and Systems*, *S82,* 664–678. Paper 63-1401.

Denn, M. (1987). *Process modelling*. New York: Wiley.

Dolezal, R., & Varcop, L. (1970). *Process dynamics*. Amstersam: Elsevier Publ. Co.

Eborn, J., & Sørlie, J. (1997). Parameter optimization of a non-linear boiler model. In Sydow, *15th IMACS world congress*, vol. 5 (pp. 725–730). Berlin, Germany: W & T Verlag.

Eklund, K. (1971). *Linear drum boiler-turbine models*. Ph.D. thesis TFRT-1001, Department of Automatic Control, Lund Institute of Technology, Lund, Sweden.

Elmqvist, H. (1978). *A structured model language for large continuous systems*. Ph.D. thesis TFRT-1015, Department of Automatic Control, Lund Institute of Technology, Lund, Sweden.

Elmqvist, H., Mattsson, S. E., & Otter, M. (1998). Modelica — the new object-oriented modeling language. In *Proceedings of the 12th european simulation multiconference* (*ESM'98*). Manchester, UK: SCS, The Society for Computer Simulation.

Garcia, C. E., Prett, D. M., & Morari, M. (1989). Model predictive control: Theory and practice — A survey. *Automatica*, *25*(3), 335–348.

Hairer, E., Lubich, C., & Roche, M. (1989). *The numerical solution of differential-algebraic systems by Runge–Kutta methods*. Lecture Notes in Mathematics, vol. 1409. Berlin: Springer.

Heusser, P. A. (1996). *Modelling and simulation of boiling channels with a general front tracking approach*. San Diego: Society for Computer Simulation, Inc.

Höld, A. (1990). UTSG — 2 a theoretical model describing the transient behavior of a pressurized water reactor natural-circulation U-tube steam generator. *Nuclear Technology*, *90*, 98–118.

Irving, E., Miossec, C., & Tassart, J. (1980). Towards efficient full automatic operation of the PWR steam generator with water level adaptive control. In *Boiler dynamics and control in nuclear power* (pp. 309–329).

Jarkovsky, J., Fessl, J., & Medulova, V. (1988). A steam generator dynamic mathematical modelling and its using for adaptive control systems testing. In *Preprints IFAC symposium on power systems modelling and control applications*. Brussels, Belgium.

Klefenz, G. (1986). *Automatic control of steam power plants* (3rd ed.). Bibliographisches Institut.

Kothare, M. V., Mettler, B., Morari, M., Bendotti, P., & Falinower, C. M. (1999). Level control in the steam generator of a nuclear power plant. *IEEE Transactions on Control Systems Technology*, to appear.

Kutateladze, S. S. (1959). *Heat transfer in condensation and boiling*. Technical Report AEC-tr-3770. United States Atomic Energy Commission.

Kwan, H. W., & Andersson, J. H. (1970). A mathematical model of a 200 MW boiler. *International Journal of Control*, *12*, 977–998.

Kwatny, H. G., & Berg, J. (1993). Drum level regulation at all loads. In *Preprints IFAC 12th world congress*, vol. 3, Sydney, Australia (pp. 405–408).

Lindahl, S. (1976). *Design and simulation of a coordinated drum boiler-turbine controller*. Lic Tech thesis TFRT-3143, Department of Automatic Control, Lund Institute of Technology, Lund, Sweden.

Lu, C. X., Bell, R. D., & Rees, N. W. (1997). Scheduling control of deaerator plant. In *Proceedings of IFAC/CIGRE symposium on control of power systems and power plants CPSPP'97*, Beijing, China (pp. 219–226). International Academic Publishers.

Maffezzoni, C. (1988). *Dinamica dei generatori di vapore*. Milano: Hartman and Braun.

Maffezzoni, C. (1992). Issues in modeling and simulation of power plants. In *Proceedings of IFAC symposium on control of power plants and power systems*, vol. 1 (pp. 19–27).

Maffezzoni, C. (1996). Boiler-turbine dynamics in power plant control. In *IFAC 13th triennial world congress*, San Francisco, USA.

Mattsson, S. E., Andersson, M., & Åström, K. J. (1993). Object-oriented modelling and simulation. In Linkens, *CAD for control systems* (pp. 31–69). New York: Marcel Dekker, Inc.

Mayne, D. Q., Rawlings, J. B., & Rao, C. V. (1999). Model predictive control: A review. *Automatica*, to appear.

McDonald, J. P., & Kwatny, H. G. (1970). A mathematical model for reheat boiler–turbine–generator systems. In *Proceedings of IEEE. PES winter power meeting*, New York. Paper 70 CP221-PWR.

McDonald, J. P., Kwatny, G. H., & Spare, J. H. (1971). A nonlinear model for reheat boiler-turbine generation systems. *Proceedings JACC* (pp. 227–236).

Menon, N. N., & Parlos, N. N. (1992). Gain-scheduled non-linear control of u-tube steam generator water level. *Nuclear Science and Engineering*, *111*, 294–308.

Miller, N., Bentsman, J., Drake, D., Fakhfakh, J., Jolly, T., Pellegrinetti, G., & Tse, J. (1990). Control of steam generation processes. In *Proceedings of ISA 90*, New Orleans, Louisiana (pp. 1265–1279).

Morton, A. J., & Price, P. H. (1977). The controllability of steam output, pressure and water level in drum boilers. *Proceedings of the Institution of Mechanical Engineers*, 75–84.

Na, M. G. (1995). Design of a stem generator water level controller via the estimation of the flow errors. *Annals of Nuclear Science and Engineering*, *22*(6), 367–376.

Na, M. G., & No, H. C. (1992). Design of an adaptive observer-based controller for the water level of steam generators. *Nuclear Engineering and Design*, *135*, 379–394.

Nicholson, H. (1964). Dynamic optimisation of a boiler. *Proceedings of IEE*, *111*, 1479–1499.

Parry, A., Petetrot, J. F., & Vivier, M. J. (1995). Recent progress in sg level control in french pwr plants. In *Proceedings of International Conference on boiler dynamics and control in nuclear powerstations* (pp. 81–88). British Nuclear Energy Society.

Pellegrinetti, G., Bentsman, J., & Polla, K. (1991). Control of nonlinear steam generation processes using h^{∞} design. In *Proceedings of 1991 ACC*, Boston, Massachusetts (pp. 1292–1297).

Profos, P. (1955). Dynamics of pressure and combustion control in steam generators. *Sulzer Technical Review 4*, V37, 1–15.

Profos, P. (1962). *Die Regelung von Dampfanlagen*. Berlin: Springer.

Qin, S. J., & Badgwell, T. A. (1997). An overview of industrial model predictive control technology. *AIChE Symposium Series*, vol. 97.

Quazza, G. (1968). Sui modelli analitici delle caldaie a corpo cilindrico. Parte I: Dinamica del vaporizzatore. *Automazione e Strumentazione,* 506–537.

Quazza, G. (1970). Automatic control in electric power systems. *Automatica*, *6*, 123–150.

Schneider, W. G., & Boyd, J. T. (1985). Steam generator level controllability. In *Boiler dynamics and control in nuclear power station* (pp. 97–117). *Proceedings Power Station 3*.

Sørlie, J., & Eborn, J. (1999). *A grey-box identification case study: The Åström-Bell Drum–boiler Model*. Technical Report. Department of Automatic Control, Lund Institute of Technology, Lund, Sweden, to appear.

Speedy, C. B., Bell, R. D., & Goodwin, G. C. (1970). Dynamic modelling of a steam generator using least squares analysis. In *Proceedings of JACC* (pp. 365–372). Atlanta, Georgia.

Thomas, P. J., Harrison, T. A., & Hollywell, P. D. (1985). Analysis of limit cycling on a boiler feedwater control system. In *Boiler dynamics and control in nuclear power station* (pp. 89–96). *Proceedings of Power Station 3*.

Thompson, F. T. (1964). *A dynamic model for control of a drum type boiler system*. Ph.D. thesis, University of Pittsburg, USA.

Tyssø, A., Brembo, J. C., & Lind, K. (1976). The design of multivariable control system for a ship boiler. *Automatica*, *12*, 211–224.

Unbehauen, H., & Kocaarslan, I. (1990). Experimental modelling and adaptive power control of a 750 MV once-through boiler. In *Preprints IFAC 11th world congress on automatic control*, vol. 11, Tallinn, Estonia (pp. 32–37).

Yeung, M. R., & Chan, P. L. (1990). Development and validation of a steam generator simulation model. *Nuclear Technology*, *92*, 309–314.

Karl J. Åström is Professor and Head of the Department of Automatic Control at Lund University since 1965. He has broad interests in automatic control including, stochastic control, system identification, adaptive control, computer control and computer-aided control engineering. He has supervised 44 Ph.D. students, written six books and more than 100 papers in archival journals. He is a member of the Royal Swedish Academy of Engineering Sciences (IVA) and the Royal Swedish Academy of Sciences (KVA) and a foreign member of the US National Academy of Engineering and the Russian Academy of Sciences. Åström has received many honors including three honorary doctorates, the Callender Silver Medal, the Quazza Medal from IFAC, the Rufus Oldenburger Medal from ASME, the IEEE Control Systems Science Award and the IEEE Medal of Honor.

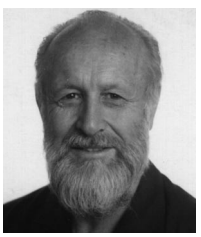

Rod Bell is an Honorary Senior Research Fellow, a position he has held since February 1998. His previous position was Head of the Computing Department which he held since the beginning of 1994. He obtained his Ph.D. (Application of Optimal Control Theory to Industrial Processes) in 1972 from the University of New South Wales. He joined the academic staff at Macquarie University in 1972. He became interested in computers (hardware and software) in 1958 when he worked on one of the first digital computers in Australia, UTECOM at the University of New South Wales. His current research interests lie mainly in the Application of Control Theory to areas such as Industrial Processes (Power Stations in particular), National Economies, Management and Robotics. He is a member of IEEE. Among his personal interests are horse riding, growing waratahs, bush walking and restoring Jaguar cars.